

# An Artificial Spiking Afferent Nerve Based on Synaptic Transistor for Thermal Perception

Sheng Li<sup>1</sup>, Jing Wu, Hanbai Lyu, Yuchen Xie, Yiqi Sun, Qinyu Chen, Yi Shi, and Lijia Pan<sup>2</sup>, *Senior Member, IEEE*

**Abstract**—The emulation of biological perception system enhances electronics via superior environmental interpretation accuracy. This research presents an artificial thermosensitive afferent nerve replicating key biological functions associated with cutaneous thermal perception, information processing, and reflex responses. The neuromorphic device integrates a thermosensitive sensor, a spiking encoder module, an ion gel-gated artificial synapse, and a spiking convolutional neural network (SCNN). This device allows precise temperature detection and initiates reflex-like responses to noxious thermal stimuli. It demonstrates high accuracy in regional temperature recognition and identification of handwritten digits (98.7%). The findings indicate a viable strategy for paving the way toward future advancements in artificial nerves, neural prosthetics, and humanoid robotics.

**Index Terms**—Artificial nerve, synaptic transistor, thermal perception, ion gel-gated, SCNN.

## I. INTRODUCTION

**H**UMANS possess complex sensorimotor systems to interact with the world. Such interaction encompasses sensing, transmitting, integrating, and processing, enabling accurate perception and timely response to stimuli [1].

Manuscript received 14 October 2023; accepted 5 November 2023. Date of publication 8 November 2023; date of current version 29 December 2023. This work was supported in part by the Scientific Research Foundation of Jiangsu Provincial Education Department under Grant 23KJB510001; in part by the Leading Innovative Talents Introduction and Cultivation Project of Changzhou under Grant CQ20220110; in part by the National Key Research and Development Program of China under Grant 2021YFA1401103; in part by the National Natural Science Foundation of China under Grant 61825403, Grant 1921005, and Grant 61674078; in part by the Jiangsu Student's Platform for Innovation and Entrepreneurship Training Program under Grant 202310292038Z; in part by the Natural Science Foundation of Jiangsu Province under Grant BK20230629; and in part by the Start-Up Funds from Changzhou University. The review of this letter was arranged by Editor P. Barquinha. (Sheng Li, Jing Wu, and Hanbai Lyu contributed equally to this work.) (Corresponding authors: Sheng Li; Qinyu Chen; Lijia Pan.)

Sheng Li and Yuchen Xie are with the School of Microelectronics and Control Engineering, Changzhou University, Changzhou 213164, China (e-mail: sli@cczu.edu.cn).

Jing Wu, Yiqi Sun, Yi Shi, and Lijia Pan are with the Collaborative Innovation Center of Advanced Microstructures, School of Electronic Science and Engineering, Nanjing University, Nanjing 210093, China (e-mail: ljpan@nju.edu.cn).

Hanbai Lyu is with the Department of Physics, Yale University, New Haven, CT 06511 USA.

Qinyu Chen is with the Institute of Neuroinformatics, University of Zurich and ETH Zurich, 8057 Zurich, Switzerland (e-mail: qinyu.chen@ini.uzh.ch).

Color versions of one or more figures in this letter are available at <https://doi.org/10.1109/LED.2023.3330961>.

Digital Object Identifier 10.1109/LED.2023.3330961

Biomimetic nerves, inspired by biological perception systems, facilitate data-parallel, energy-efficient, and fault-tolerant operations in artificial systems [2], [3]. These biomimetic nerves introduce a unique computing paradigm that merges perception, storage, and computation. Moreover, these artificial systems encompass multiple human-like perception functions including vision [4], [5], [6], [7], hearing [8], [9], [10], touch [11], [12], [13], [14], and even taste [15]. They have the potential to circumvent the von Neumann bottleneck, paving the way for significant advancements in humanoid robotics, neural prosthetics, and human-machine interfaces [16], [17].

Biological peripheral nerves perceive external information using multimodal receptors. Assisted by synapses, the spinal cord, and the brain, temporal data are efficiently synthesized and interpreted as spike sequences. Thermal sensation, a fundamental human sensory, transduces ambient temperature information via peripheral nerves [18]. As shown in Fig. 1(a), thermosensitive afferents respond to thermal stimuli; their discharge frequency increases with rising temperatures [19]. Thermoception is generated after being transmitted to the somatosensory cortex through billions of synapses. When exposed to painful heat (above 55 °C), the spinal cord initiates a rapid reflex action. This protective mechanism is further modulated by the brain [20], [21], [22]. To replicate this perception mechanism, biomimetic sensory systems are typically developed by integrating neuromorphic devices with sensors [23], [24], [25], [26].

In this letter, we introduce an artificial thermosensitive afferent nerve that is capable of temperature sensing, spike encoding, and neuromorphic computing. This device can accurately detect ambient thermal values within a specified range for a single hotspot and can initiate a reflex-like response when exposed to noxious heat. Additionally, it successfully identifies thermal stimulation areas and recognizes digit patterns.

## II. EXPERIMENT DETAILS

**Fabrication of the Thermal Receptor:** Silver ink (75 wt%) was screen printed and annealed at 65 °C on a PET substrate to form electrodes. A precursor solution was prepared by mixing PEDOT:PSS (1.3 wt%) with CNTs (231:1 wt ratio) and was ultrasonically spray coated to form the sensitive layer. A parylene C layer was then deposited as a package layer.

**Fabrication of the Synaptic Transistor:** The IGZO channel (30 nm) and ITO electrodes (100 nm) were deposited on a transparent glass substrate using magnetron sputtering. The precursor for the ionic gel was prepared by mixing polyethylene glycol diacrylate (PEGDA) monomer, 2-hydroxy-2-methylpropiophenone (HOMPP) photoinitiator,

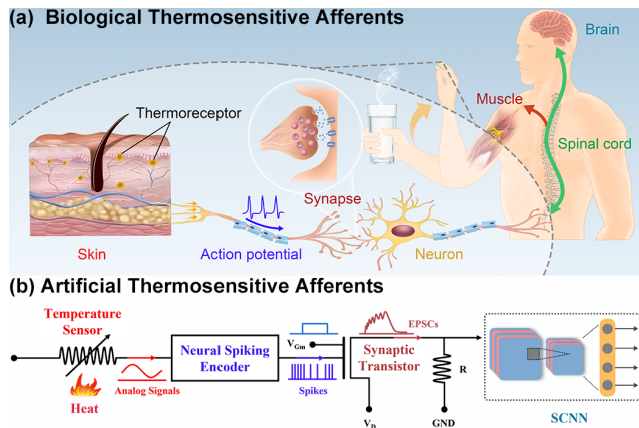


Fig. 1. (a) Schematic of the biological thermosensitive afferents. (b) Schematic diagram of the artificial thermosensitive afferents.

and [EMIM][TFSI] ionic liquid (6:3:11 wt ratio). This mixture was then drop casted and UV polymerized to form a dielectric layer.

**Fabrication of the Spiking Encoder Module:** This customized module primarily consists of an integrator, a hysteresis comparator, and a zero-crossing comparator. It was realized on a circuit board.

Electrical properties are acquired on Keithley 4200A-SCS.

### III. RESULTS AND DISCUSSION

This artificial afferent nerve incorporates a temperature sensor, a spiking encoder module and a synaptic transistor (Fig. 1(b)). The temperature sensor acts as a thermoreceptor, with the spiking encoder functioning as a nerve fiber to translate thermal stimuli into voltage spikes. These signals are then converted into postsynaptic currents by the synaptic transistor and further processed by the SCNN. The temperature sensor is composed of silver electrodes, a PEDOT:PSS/CNTs thermo-sensitivity layer, and a parylene encapsulation layer. The temperature-sensitive characteristics primarily arise from the core-shell microstructure of PEDOT:PSS, where a PEDOT nanocrystal forms the core, encased by a PSS shell [27]. The bulk resistivity is largely influenced by the insulating PSS boundaries. As thermal stimuli increase, the boundary between the polymer particles contracts, resulting in a decrease in resistance. Conversely, at lower temperature, there's insufficient thermal energy for electrons to traverse the PSS boundary, leading to a rise in overall resistance. CNTs, another intrinsically temperature-sensitive material with outstanding electrical conductivity, further boosts electron hopping at the interface [28]. Human typically feel warmth when temperatures exceed 33°C [22]. As such, our sensor was tested in the range of 33 to 88 °C. Linear I-V characteristics is observed (Fig. 2(a)). Fig. 2(b) showcases the normalized resistance change ( $\Delta R/R_0$ ) with increasing temperature. The calculated sensitivity is approximately 0.87 %/°C, which is superior to sensors utilizing solely PEDOT:PSS (0.4 %/°C) or CNTs (0.29 %/°C) [29], [30].

The neural spiking encode module translates external stimuli into artificial neural spikes. The circuit diagram of this module is shown in Fig. 2(e), comprising an integrator ( $U_1$ ), a hysteresis comparator ( $U_2$ ), and a zero-crossing comparator ( $U_3$ ). An increase in input voltage leads to a higher frequency of output spikes without significantly changing the amplitude.

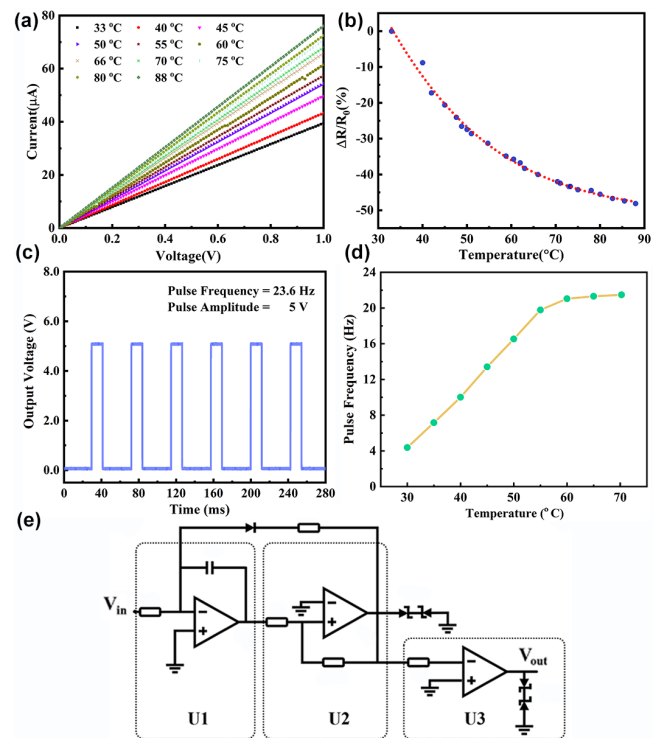


Fig. 2. (a) I-V characteristics of the temperature sensor. (b) Normalized resistance changes as a function of temperature. (c) A typical encoded spiking sequence. (d) The frequency of encoded spikes as a function of temperature. (e) The circuit diagram of the spiking encoder module.

This frequency range is consistent with biological receptors, ranging from zero to several dozens of Hz [21]. Fig. 2(c) displays typical encoded spikes with a frequency of 23.6 Hz and a consistent amplitude of 5 V. To mimic a biological warm fiber, a temperature sensor and encoder are interconnected. The firing rate surges within 30-55 °C, and begins to stabilize beyond 55 °C (Fig. 2(d)). This behavior aligns with biological thermosensitive afferents, which perceive stimuli at 55 °C as painful and subsequently inhibit further nerve excitation [31].

An ion gel-gated synaptic transistor is designed to emulate the biological synapse (Fig. 3(a)). A gate (G) and source/drain (S/D) electrodes functions as pre-synaptic and postsynaptic output terminals. A modulatory gate ( $G_m$ ) regulates the overall behavior, resembling the descending pathway [32], [33]. Fig. 3(b) shows the transfer curves at  $V_{DS} = 0.2$  V. A high on/off ratio of  $\sim 3 \times 10^4$  is exhibited. An obvious hysteresis loop is due to the slow drift process of ions [34]. This device emulates the paired-pulse facilitation (PPF) under two pulses with the same amplitude ( $V_G = 5$  V) at  $V_{DS} = 0.2$  V (Fig. 3(c)). Fig. 3(d) presents the PPF index ( $100\% \times A_2/A_1$ ) as a function of spike interval ( $\Delta t$ ). A typical PPF index of  $\approx 200\%$  is obtained at  $\Delta t = 90$  ms and this ratio declines gradually as  $\Delta t$  rises. Dynamic high-pass temporal filtering is also emulated by this device, as shown in Fig. 3(e). The spike sequences applied on the gate consist of 10 spikes with a fixed amplitude of 5 V with various frequencies, at  $V_{DS} = 0.2$  V.  $V_{Gm}$  regulates the synaptic plasticity, and excitatory postsynaptic currents (EPSCs) is potentiated under a positive bias, while depressed under a negative bias, at  $V_{DS} = 0.2$  V and  $V_G = 5$  V (Fig. 3(f)). The synaptic weight change ( $\Delta W$ ) is calculated by  $\Delta W = (A_2 - A_1)/A_1$ , where  $A_1$  and  $A_2$  are the initial and final amplitude of EPSC. At  $V_{Gm} = 0.5$  V,  $\Delta W$

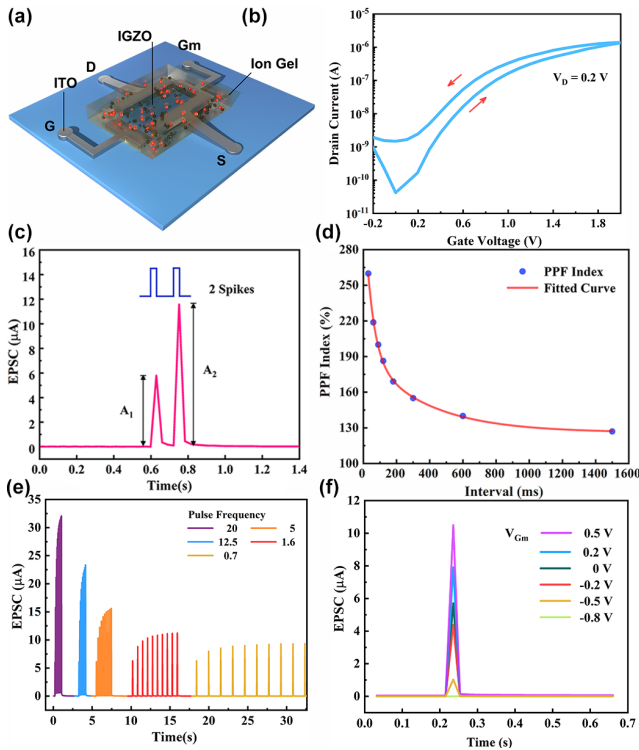


Fig. 3. (a) Schematic diagram of the synaptic transistor. (b) Transfer characteristic. (c) Typical PPF phenomenon. (d) PPF index as a function of spike time interval. EPSCs under spikes with various frequency (e) and  $V_{Gm}$  (f).

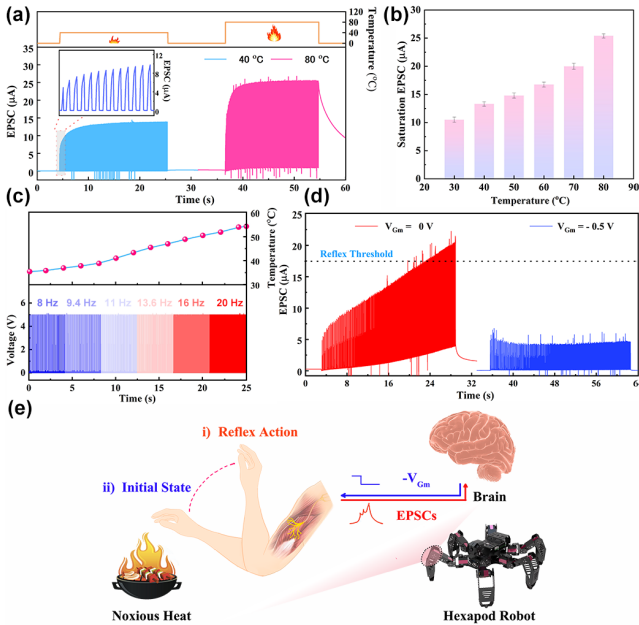


Fig. 4. (a) EPSCs generated at 40 and 80 °C. (b) The saturation EPSC under various temperatures. (c) Spikes generated from the encoder from 35 to 55 °C. (d) EPSCs under dynamic thermal stimuli by applying various  $V_{Gm}$ . (e) Working mechanism of an implanted artificial nerve.

enhances significantly to  $\sim 90\%$ , while at  $V_{Gm} = -0.8$  V, the synaptic plasticity is repressed obviously.

Our artificial afferent device is sensitive to both steady-state or transient thermal stimuli, analogous to human afferents [18]. Fig. 4(a) illustrates two series of EPSCs at 40 °C and 80 °C. Thermal stimuli initiate consecutive impulses and activate the transistor subsequently. According to the characteristics of the spiking encoder, the spikes are generated with a fixed

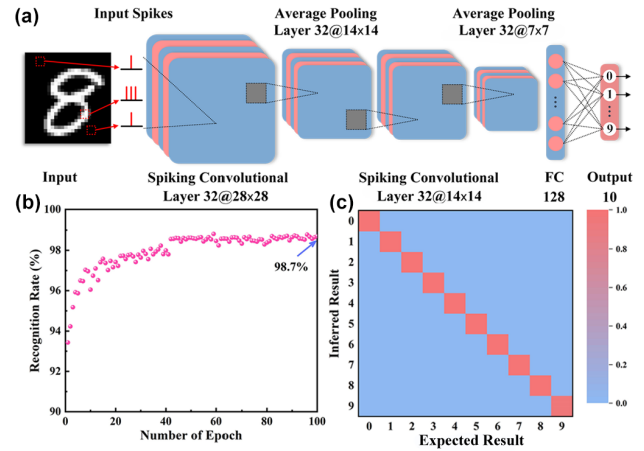


Fig. 5. (a) Schematic of the SCNN for pattern recognition. (b) The recognition rate versus the number of epochs. (c) Confusion matrix of the test results.

amplitude of 5 V and various frequency. Under a  $V_{DS}$  of 0.2 V, EPSCs escalates from 6  $\mu$ A to saturation values of 14 and 25  $\mu$ A, and the saturation value is highly responsive to the ambient temperature from 30 to 80 °C (Fig. 4(b)). Biological nerve also responds rapidly to dynamic thermal stimuli [35]. Our device is integrated into a hexapod robot (Fig. 4(e)). A comparator compares EPSCs with a preset threshold, and an analog switch serves as a biological spine, transmitting motion signals generated from CPU. Upon encountering noxious heat, rapidly increasing EPSCs activate the switch to execute pre-stored reflex. This process can also be adjusted through  $V_{Gm}$  from CPU. As ambient temperature rises from 35 to 55 °C, the frequency of spiking impulses increases from 8 to 20 Hz (Fig. 4(c)), following an increase in EPSCs (Fig. 4(d)). It takes about 20 seconds to exceed the threshold (17.5  $\mu$ A), activating a reflex. The device also exhibits an inhibition function under negative  $V_{Gm}$ . Heat is tolerated, and reflex action is inhibited. The results confirm that this artificial nerve, once integrated into robotics, can successfully realize biomimic ambient thermal perception and unconditional reflex.

Human skin is able to detect thermal information from specific areas, enabling individuals to roughly discern patterns, contours, or objects [22]. We designed a SCNN to recognize handwritten digits, leveraging the MNIST dataset. The architecture of the SCNN is illustrated in Fig. 5(a), where digit-pattern recognition based on thermal perception is achieved. The SCNN training starts from the experimentally measured electrical characteristics shown in Fig. 2(d), and additional data is generated via interpolation. Fig. 5(b) charts the progression of the recognition rate across training epochs. Classification accuracy peaks at 98.7% after 100 training epochs. Fig. 5c showcases a normalized confusion matrix, where a pronounced diagonal pattern indicates accurate recognition of the handwritten digits.

#### IV. CONCLUSION

We introduced an artificial thermosensitive afferent nerve that excels in precise thermal detection for both individual hotspots and larger stimulation areas. This innovation achieves high accuracy in digit-pattern recognition. Furthermore, our work holds significant potential to drive advancements in neural prosthetics, implantable electronics, and humanoid robotics.

## REFERENCES

- [1] C. Jiang, J. Liu, Y. Ni, S. Qu, L. Liu, Y. Li, L. Yang, and W. Xu, "Mammalian-brain-inspired neuromorphic motion-cognition nerve achieves cross-modal perceptual enhancement," *Nature Commun.*, vol. 14, no. 1, p. 1344, Mar. 2023, doi: [10.1038/s41467-023-36935-w](https://doi.org/10.1038/s41467-023-36935-w).
- [2] Y. Sun, J. Li, S. Li, Y. Jiang, E. Wan, J. Zhang, Y. Shi, and L. Pan, "Advanced synaptic devices and their applications in biomimetic sensory neural system," *Chip*, vol. 2, no. 1, Mar. 2023, Art. no. 100031, doi: [10.1016/j.chip.2022.100031](https://doi.org/10.1016/j.chip.2022.100031).
- [3] L. Sun et al., "An artificial reflex arc that perceives afferent visual and tactile information and controls efferent muscular actions," *Research*, vol. 2022, Jan. 2022, Art. no. 9851843, doi: [10.34133/2022/9851843](https://doi.org/10.34133/2022/9851843).
- [4] S. Li, H. Lyu, Y. Zhou, H. Wang, J. Wu, X. Gao, J. Li, Q. Wan, D. Kong, Y. Shi, and L. Pan, "Artificial reflex arc: An environment-adaptive neuromorphic camouflage device," *IEEE Electron Device Lett.*, vol. 42, no. 8, pp. 1224–1227, Aug. 2021, doi: [10.1109/LED.2021.3090767](https://doi.org/10.1109/LED.2021.3090767).
- [5] Q.-B. Zhu, B. Li, D.-D. Yang, C. Liu, S. Feng, M.-L. Chen, Y. Sun, Y.-N. Tian, X. Su, X.-M. Wang, S. Qiu, Q.-W. Li, X.-M. Li, H.-B. Zeng, H.-M. Cheng, and D.-M. Sun, "A flexible ultrasensitive optoelectronic sensor array for neuromorphic vision systems," *Nature Commun.*, vol. 12, no. 1, p. 1798, Mar. 2021, doi: [10.1038/s41467-021-22047-w](https://doi.org/10.1038/s41467-021-22047-w).
- [6] C. Chen, Y. He, H. Mao, L. Zhu, X. Wang, Y. Zhu, Y. Zhu, Y. Shi, C. Wan, and Q. Wan, "A photoelectric spiking neuron for visual depth perception," *Adv. Mater.*, vol. 34, no. 20, May 2022, Art. no. 2201895, doi: [10.1002/adma.202201895](https://doi.org/10.1002/adma.202201895).
- [7] C. Wan, P. Cai, X. Guo, M. Wang, N. Matsuhisa, L. Yang, Z. Lv, Y. Luo, X. J. Loh, and X. Chen, "An artificial sensory neuron with visual-haptic fusion," *Nature Commun.*, vol. 11, no. 1, p. 4602, Sep. 2020, doi: [10.1038/s41467-020-18375-y](https://doi.org/10.1038/s41467-020-18375-y).
- [8] S. Das, A. Dodda, and S. Das, "A biomimetic 2D transistor for audiomorphic computing," *Nature Commun.*, vol. 10, no. 1, p. 3450, Aug. 2019, doi: [10.1038/s41467-019-11381-9](https://doi.org/10.1038/s41467-019-11381-9).
- [9] S. Seo, B.-S. Kang, J.-J. Lee, H.-J. Ryu, S. Kim, H. Kim, S. Oh, J. Shim, K. Heo, S. Oh, and J.-H. Park, "Artificial van der Waals hybrid synapse and its application to acoustic pattern recognition," *Nature Commun.*, vol. 11, no. 1, p. 3936, Aug. 2020, doi: [10.1038/s41467-020-17849-3](https://doi.org/10.1038/s41467-020-17849-3).
- [10] Y. He, S. Nie, R. Liu, S. Jiang, Y. Shi, and Q. Wan, "Spatiotemporal information processing emulated by multiterminal neuro-transistor networks," *Adv. Mater.*, vol. 31, no. 21, May 2019, Art. no. 1900903, doi: [10.1002/adma.201900903](https://doi.org/10.1002/adma.201900903).
- [11] F. Yu, J. C. Cai, L. Q. Zhu, M. Sheikhi, Y. H. Zeng, W. Guo, Z. Y. Ren, H. Xiao, J. C. Ye, C.-H. Lin, A. B. Wong, and T. Wu, "Artificial tactile perceptual neuron with nociceptive and pressure decoding abilities," *ACS Appl. Mater. Interfaces*, vol. 12, no. 23, pp. 26258–26266, Jun. 2020, doi: [10.1021/acsami.0c04718](https://doi.org/10.1021/acsami.0c04718).
- [12] C. Zhang, S. Li, Y. He, C. Chen, S. Jiang, X. Yang, X. Wang, L. Pan, and Q. Wan, "Oxide synaptic transistors coupled with triboelectric nanogenerators for bio-inspired tactile sensing application," *IEEE Electron Device Lett.*, vol. 41, no. 4, pp. 617–620, Apr. 2020, doi: [10.1109/LED.2020.2972038](https://doi.org/10.1109/LED.2020.2972038).
- [13] X. Wu, E. Li, Y. Liu, W. Lin, R. Yu, G. Chen, Y. Hu, H. Chen, and T. Guo, "Artificial multisensory integration nervous system with haptic and iconic perception behaviors," *Nano Energy*, vol. 85, Jul. 2021, Art. no. 106000, doi: [10.1016/j.nanoen.2021.106000](https://doi.org/10.1016/j.nanoen.2021.106000).
- [14] D. W. Kim, J. C. Yang, S. Lee, and S. Park, "Neuromorphic processing of pressure signal using integrated sensor-synaptic device capable of selective and reversible short- and long-term plasticity operation," *ACS Appl. Mater. Interfaces*, vol. 12, no. 20, pp. 23207–23216, May 2020, doi: [10.1021/acsami.0c03904](https://doi.org/10.1021/acsami.0c03904).
- [15] L. Yang, Z. Wang, S. Zhang, Y. Li, C. Jiang, L. Sun, and W. Xu, "Neuromorphic gustatory system with salt-taste perception, information processing, and excessive-intake warning capabilities," *Nano Lett.*, vol. 23, no. 1, pp. 8–16, Jan. 2023, doi: [10.1021/acs.nanolett.2c02775](https://doi.org/10.1021/acs.nanolett.2c02775).
- [16] S. Li, Z. Ma, Z. Cao, L. Pan, and Y. Shi, "Advanced wearable microfluidic sensors for healthcare monitoring," *Small*, vol. 16, no. 9, Mar. 2020, Art. no. 1903822, doi: [10.1002/sml.201903822](https://doi.org/10.1002/sml.201903822).
- [17] Y. Ni, L. Liu, J. Liu, and W. Xu, "A high-strength neuromuscular system that implements reflexes as controlled by a multiquadrant artificial efferent nerve," *ACS Nano*, vol. 16, no. 12, pp. 20294–20304, Dec. 2022, doi: [10.1021/acsnano.2c06122](https://doi.org/10.1021/acsnano.2c06122).
- [18] S. A. Prescott and S. Ratte, "Somatosensation and pain," in *Conn's Translational Neuroscience*. Cambridge, MA, USA: Academic Press, 2017, pp. 517–539, doi: [10.1016/B978-0-12-802381-5.00037-3](https://doi.org/10.1016/B978-0-12-802381-5.00037-3).
- [19] A. Teliban, F. Bartsch, M. Struck, R. Baron, and W. Jänig, "Axonal thermosensitivity and mechanosensitivity of cutaneous afferent neurons," *Eur. J. Neurosci.*, vol. 33, no. 1, pp. 110–118, Jan. 2011, doi: [10.1111/j.1460-9568.2010.07471.x](https://doi.org/10.1111/j.1460-9568.2010.07471.x).
- [20] A. Iggo, "Cutaneous thermoreceptors in primates and sub-primates," *J. Physiol.*, vol. 200, no. 2, pp. 403–430, Feb. 1969, doi: [10.1113/jphysiol.1969.sp008701](https://doi.org/10.1113/jphysiol.1969.sp008701).
- [21] H. Hensel, "Thermoreceptors," *Annu. Rev. Physiol.*, vol. 36, no. 1, pp. 233–249, Mar. 1974, doi: [10.1146/annurev.ph.36.030174.001313](https://doi.org/10.1146/annurev.ph.36.030174.001313).
- [22] R. J. Schepers and M. Ringkamp, "Thermoreceptors and thermosensitive afferents," *Neurosci. Biobehavioral Rev.*, vol. 34, no. 2, pp. 177–184, Feb. 2010, doi: [10.1016/j.neubiorev.2009.10.003](https://doi.org/10.1016/j.neubiorev.2009.10.003).
- [23] H. Tan, Q. Tao, I. Pande, S. Majumdar, F. Liu, Y. Zhou, P. O. Å. Persson, J. Rosen, and S. van Dijken, "Tactile sensory coding and learning with bio-inspired optoelectronic spiking afferent nerves," *Nature Commun.*, vol. 11, no. 1, p. 1369, Mar. 2020, doi: [10.1038/s41467-020-15105-2](https://doi.org/10.1038/s41467-020-15105-2).
- [24] H. Wei, R. Shi, L. Sun, H. Yu, J. Gong, C. Liu, Z. Xu, Y. Ni, J. Xu, and W. Xu, "Mimicking efferent nerves using a graphdiyne-based artificial synapse with multiple ion diffusion dynamics," *Nature Commun.*, vol. 12, no. 1, p. 1068, Feb. 2021, doi: [10.1038/s41467-021-21319-9](https://doi.org/10.1038/s41467-021-21319-9).
- [25] C. Zhang, W. B. Ye, K. Zhou, H. Chen, J. Yang, G. Ding, X. Chen, Y. Zhou, L. Zhou, F. Li, and S. Han, "Bioinspired artificial sensory nerve based on Nafion memristor," *Adv. Funct. Mater.*, vol. 29, no. 20, May 2019, Art. no. 1808783, doi: [10.1002/adfm.201808783](https://doi.org/10.1002/adfm.201808783).
- [26] S. Li, H. Lyu, J. Li, Y. He, X. Gao, Q. Wan, Y. Shi, and L. Pan, "Multiterminal ionic synaptic transistor with artificial blink reflex function," *IEEE Electron Device Lett.*, vol. 42, no. 3, pp. 351–354, Mar. 2021, doi: [10.1109/LED.2021.3051645](https://doi.org/10.1109/LED.2021.3051645).
- [27] T. Takano, H. Masunaga, A. Fujiwara, H. Okuzaki, and T. Sasaki, "PEDOT nanocrystal in highly conductive PEDOT:PSS polymer films," *Macromolecules*, vol. 45, no. 9, pp. 3859–3865, May 2012, doi: [10.1021/ma300120g](https://doi.org/10.1021/ma300120g).
- [28] S. Gong, Z. H. Zhu, and Z. Li, "Electron tunnelling and hopping effects on the temperature coefficient of resistance of carbon nanotube/polymer nanocomposites," *Phys. Chem. Chem. Phys.*, vol. 19, no. 7, pp. 5113–5120, 2017, doi: [10.1039/C6CP08115K](https://doi.org/10.1039/C6CP08115K).
- [29] W. Honda, S. Harada, T. Arie, S. Akita, and K. Takei, "Wearable, human-interactive, health-monitoring, wireless devices fabricated by macroscale printing techniques," *Adv. Funct. Mater.*, vol. 24, no. 22, pp. 3299–3304, Jun. 2014, doi: [10.1002/adfm.201303874](https://doi.org/10.1002/adfm.201303874).
- [30] W. Honda, S. Harada, T. Arie, S. Akita, and K. Takei, "Printed wearable temperature sensor for health monitoring," in *Proc. IEEE SENSORS*, Nov. 2014, pp. 2227–2229, doi: [10.1109/ICSENS.2014.6985483](https://doi.org/10.1109/ICSENS.2014.6985483).
- [31] J. Van Hees and J. Gybels, "C nociceptor activity in human nerve during painful and non painful skin stimulation," *J. Neurol., Neurosurgery Psychiatry*, vol. 44, no. 7, pp. 600–607, Jul. 1981, doi: [10.1136/jnnp.44.7.600](https://doi.org/10.1136/jnnp.44.7.600).
- [32] K. H. Lee, M. S. Kang, S. Zhang, Y. Gu, T. P. Lodge, and C. D. Frisbie, "'Cut and stick' rubbery ion gels as high capacitance gate dielectrics," *Adv. Mater.*, vol. 24, no. 32, pp. 4457–4462, Aug. 2012, doi: [10.1002/adma.201200950](https://doi.org/10.1002/adma.201200950).
- [33] Y. H. Liu, L. Q. Zhu, P. Feng, Y. Shi, and Q. Wan, "Freestanding artificial synapses based on laterally proton-coupled transistors on chitosan membranes," *Adv. Mater.*, vol. 27, no. 37, pp. 5599–5604, Oct. 2015, doi: [10.1002/adma.201502719](https://doi.org/10.1002/adma.201502719).
- [34] J. Lee, L. G. Kaake, J. H. Cho, X.-Y. Zhu, T. P. Lodge, and C. D. Frisbie, "Ion gel-gated polymer thin-film transistors: Operating mechanism and characterization of gate dielectric capacitance, switching speed, and stability," *J. Phys. Chem. C*, vol. 113, no. 20, pp. 8972–8981, May 2009, doi: [10.1021/jp901426e](https://doi.org/10.1021/jp901426e).
- [35] D. Fiala and L. Univ, "Dynamic simulation of human heat transfer and thermal comfort," Doctoral dissertation, Inst. Energy Sustain. Develop., De Montfort Univ., Leicester, U.K., Jan. 1998.